Planck Motion Theory

Andrew Vida

Independent researcher, Elkview, West Virginia

ORCID: 0009-0009-2573-2914

Email: avida@protonmail.com — impublius@gmail.com

July 10, 2025

Abstract

Planck Motion Theory (PMT) proposes that motion, time, and energy are emergent phenomena arising from the discrete actions of massless, structureless units called Planck Objects (POs). These units occupy a fixed cubic lattice at Planck-scale resolution and transition between adjacent cells in discrete time steps. This abstract substrate dispenses with the continuum assumptions of classical physics and replaces them with a minimal, self-contained, and discrete causal structure. Tier 1 of PMT establishes the foundational geometry and temporal rules of this substrate, introduces the principle of Planck Motion, and formulates a completeness theorem ensuring that all valid dynamics occur entirely within the closed lattice without invoking classical convergence. This tier provides the axiomatic groundwork upon which all higher-order behavior—including mass, inertia, and wavefront propagation—emerges.

PMT aims to unify quantum mechanics and relativity through a discrete causal structure, offering testable predictions at Planck scales.

Keywords: discrete spacetime; Planck scale; cellular automaton; emergence

Notation And Glossary

Symbol	Meaning / Definition
ℓ_p	Planck length; edge length of one cubic lattice cell ($\sim 1.616 \times 10^{-35}$ m).
t_p	Planck time; one lattice "tick", $t_p = \ell_p / c$ ($\sim 5.39 \times 10^{-44}$ s).
f_p	Planck frequency, $f_p = 1/t_p \approx 1.854\,888 \times 10^{43}$ Hz; maximal PO event rate.
z (z-index)	Integer timing phase of a PO or sub-structure; determines *when* a jump is allowed.
ζ (zeta-index)	Spatial/topographic descriptor of an aggregate; determines *which* POs jump and *where*.
$\mathcal{Z} = (z, \zeta)$	Combined *z-complex*; full spatiotemporal state of an aggregate.
N_{rest}	Extra rest ticks inserted between successive jumps of a PO or aggregate wavefront.
Q	Coupling polarity (Tier 4); integer budget of outward–minus–inward phase shifts per cycle.
γ	Discrete Lorentz factor, $\gamma = (n_{\text{rest}} + \Delta n + 1)/(n_{\text{rest}} + 1)$.
Φ, $\mathbf{E}$, $\mathbf{B}$	Coarse-grained timing-front density and its discrete gradients (Tier 8 field analogues).
λ_{coh}	Coherence length: distance a coordination front can travel before decohering.
p_{jit}, p_{coup}	Probabilities per tick for timing jitter and coupling fluctuation (Tier 6).
η	Replication fidelity per cycle in an autocatalytic network (Tier 11).

Contents

0. Introduction

Planck Motion Theory (PMT) is a bottom-up physical model grounded in the premise that all observable phenomena, motion, mass, energy, time, etc., emerge from a discrete, structureless substrate composed of massless entities called Planck Objects (POs).

For the purposes of conveying the essential ideas underpinning PMT, each PO is described as a cubic structure occupying a single cubic cell of a "substrate" lattice the sides of which are of length ℓ_p[1]. The cube was chosen because it tiles perfectly without gaps or overlaps smaller than ℓ_p. One problem arising from the use of cubic geometry is that of anisotropy. A spherical configuration would have been more suitable for the sake of isotropy, but would not tile perfectly. Therefore, a compromise had to be made for the sake of clarity, and the cubic illustrative geometry was chosen. It must be clearly understood that at this time, reality at the Planck scale can only be surmised speculatively and that the theory opens vast and very fertile fields for further development and experimentation.

Practical isotropy. Even if the underlying cubic tiling is locally anisotropic, central–limit averaging over orientation domains of size $\ell_d \sim 10^{2\text{–}3}\,\ell_p$ suppresses residual light-speed variation as $(\ell_d/L)^{3/2}$ (App. A.4). For laboratory baselines $L \gtrsim 1$ fm the expected $\Delta c/c \lesssim 10^{-22}$ is already below current Michelson–Morley bounds, so Planck-scale anisotropy is experimentally invisible at quantum and classical scales.

Similarly, time advances in discrete intervals of t_p. Motion is defined as an *instantaneous* jump from one cell to an adjacent one, which necessarily follows if the notion of Planck-length is to be assumed to hold in reality. This, of course, raises the apparent issue of infinite velocity. This apparent paradox is resolved by introducing a mandatory rest interval after jumping from one cell to another for an absolute minimal interval of one t_p, establishing the unit behavior known as Planck motion. A PO resting for one t_p after every jump will advance at the speed of light. POs that rest for more than one t_p advance at less than the speed of light.

Unlike continuum-based theories that rely on differential structures and real-number topology, PMT asserts that all physically real positions and times are integer multiples of these fundamental units. This discretized ontology eliminates the need for limit processes, calculus-based dynamics, or continuous fields at the foundational level. Instead, behavior arises through local discrete interactions governed by deterministic or probabilistic transition rules unique to each level of organizational complexity of POs, which are assumed to be *self-organizing* as a matter of their inherent nature.

PMT assumes that POs will self-organize at the most fundamental level, congealing into aggregate objects. When such an organization stabilizes locally, for any given size of a specific locality, then by the same self-organizing nature they will further organize into yet more complex aggregates. Aggregates of a given level bear their unique characteristics that establish the set of rules of behavior for that level. Once a level of organization stabilizes,

the process repeats itself, each level of organization building new complexities upon those of the previous level or perhaps even levels.

At the Planck scale, PMT theorizes that none of the phenomena commonly regarded as fundamental in conventional models exists as we know them, even at the quantum scale. There exists no time as we conceive it, nor is there gravity, mass, inertia, momentum, charge, weak or strong force, or any force at all. All these phenomena are emergent as a result of how PO aggregates are structured and how they operate at their respective levels.

PMT models motion as a set of statistical probabilities. Because the PO is so small and their quantities so enormous, the statistical law of large numbers implies that what we observe as continuity is actually vast numbers of POs moving discretely through space and time, the mesh so fine that reality becomes effectively continuous in terms of our experience of it. This macroscopic regularity, arising from probabilistic dynamics, invites a framework capable of expressing superposition, coherence, and phase relationships—traits not easily handled by purely discrete models.

This probabilistic framework may allow certain aggregate behaviors in PMT to be represented as vectors or operators within Hilbert spaces, especially when modeling coherent wavefront propagation. In this light, the law of large numbers can be interpreted as a type of statistical convergence analogous to weak convergence in functional spaces. While PMT itself is a fundamentally discrete theory, it may give rise to a Hilbert-space-like structure at higher levels of organization where aggregate wave phenomena dominate.

As the complexity of PO aggregates grows, there would eventually evolve a layer at which the organization is such that we can observe composite and elementary particles such as gluons, bosons, electrons, and protons. This organizational stability, facilitated by the law of large numbers, ensures that aggregate behaviors converge toward stable statistical profiles—making it possible for known particles to emerge from an otherwise stochastic substrate.

PMT is structured into twelve tiers, each building hierarchically on the ones prior.

Tier 1 *Foundational Structure*: Defines the discrete substrate, axiomatic motion rules, and completeness conditions.

Tier 2 *Aggregation and Internal Constraints*: Describes how Planck Objects form stable aggregates and how internal coordination limits propagation.

Tier 3 *Emergent Properties*: Introduces mass, inertia, and coherence as statistical outcomes of aggregate structure.

Tier 4 *Wavefront Propagation*: Explains how motion occurs at the composite level through staggered transitions.

Tier 5 *Relativistic Behavior*: Derives time dilation and Lorentz-like effects from internal delays within the lattice.

Tier 6 *Probabilistic Dynamics*: Introduces the role of stochastic processes in long-term evolution and configuration collapse.

Tier 7 *Measurement and Observation*: Models decoherence, observer interaction, and statistical resolution of configurations.

Tier 8 *Field Analogues*: Describes how aggregate ensembles give rise to field-like behaviors.

Tier 9 *Macroscopic Structure*: Builds toward composite systems including atoms, molecules, and bulk matter.

Tier 10 *Complex Systems and Life*: Discusses emergent biological structure and dynamic feedback from embedded information.

Tier 11 *Consciousness and Top-Down Influence*: Explores speculative models for mind-body interaction through aggregate state modulation.

Tier 12 *Cosmology and Boundary Conditions*: Frames the global structure of the substrate, initial conditions, and system finiteness.

Tier 1 establishes the discrete ontological foundation of PMT. The substrate consists of massless, indistinguishable Planck Objects (POs) occupying a perfectly tiled cubic lattice, where each PO resides in a cell of side ℓ_p and may jump instantaneously to a neighboring cell, then rest for at least t_p. This motion defines the concept of Planck Motion. Time and distance are not continuous, but discretized into integral multiples of these units. Tier 1 formulates a completeness theorem (PMT-Completeness) that proves the substrate is internally sufficient and closed: all admissible sequences of PO behavior stabilize, terminate, or repeat entirely within the system, without reference to external structures or classical convergence. These principles establish the immutable operating framework upon which all higher-tier structures and dynamics must be built.

Tier 1 introduces a theorem of PMT-completeness, which ensures that all valid physical dynamics take place entirely within this discrete structure—there is no need for external embedding, boundary conditions, or classical convergence. The rules summarized in this tier define the immutable operating principles from which all higher-level structures—including aggregate objects, coherence, inertia, and spacetime curvature—must emerge.

This foundation supports a broader program to derive known physical laws from discrete combinatorial and coordination delays, providing a testable alternative to both quantum field theory and general relativity at Planck scales.

This tier also supports a harmonic interpretation of hierarchical emergence: the aggregate structures and behaviors that arise in higher tiers may be understood as successive reductions in frequency from the fundamental Planck rate. The Planck frequency, representing the maximum event rate per PO, serves as a base harmonic, and all higher-level dynamics emerge as lower harmonics—effectively an inverted Fourier hierarchy. More complex configurations exhibit richer modal structures but lower base frequencies, reflecting their greater internal

coordination demands. This harmonic layering provides a natural framework for interpreting how classical wave phenomena, including fields and particles, arise from discrete transitions without invoking a continuum.

The Planck frequency is defined as the reciprocal of the Planck time: $f_p = \frac{1}{t_p}$. It represents the highest possible transition rate for a Planck Object, and thus defines the upper bound of temporal resolution in the PMT framework. All emergent frequencies, from particle oscillations to classical waveforms, are constrained to be harmonics or sub-harmonics of this base rate.

Tier 2 addresses how Planck Objects (POs), which are inherently structureless and massless, may form stable aggregates through temporal or spatial coordination. These aggregates are composed of multiple POs that obey shared timing constraints, resulting in coherent multi-PO units. Tier 2 introduces the principle that internal coordination imposes limitations on mobility: while a free PO can move at the maximum discrete speed of $c = \ell_p/t_p$, aggregates cannot. Their propagation rate is bounded by internal synchronization demands, leading to emergent velocity constraints. This tier also formalizes the concept of dependency graphs among POs within an aggregate, laying the foundation for emergent behaviors like coherence, inertia, and system memory. It transitions PMT from the individual-object regime of Tier 1 to the collective dynamics that underpin higher-order physical structures.

Tier 3 develops the emergent properties that arise from the structure and behavior of aggregates defined in Tier 2. While POs are massless and incapable of storing energy individually, certain configurations of POs within aggregates exhibit statistical persistence and coherence over time. These properties give rise to emergent quantities such as mass, momentum, and inertia.

Mass in PMT is not a fundamental property but an emergent measure of the coordination effort required to maintain internal timing constraints within an aggregate. Aggregates that demand more internal synchronization exhibit higher effective inertia and greater resistance to changes in motion. Similarly, momentum is modeled not as a primitive vector but as a relational descriptor of aggregate propagation through the substrate, governed by the cumulative coordination cost distributed over directionally consistent transitions.

Tier 3 formalizes the statistical mechanics of aggregates, establishing rules for when coherent patterns persist and how perturbations lead to configuration changes or decoherence. These patterns become the precursors to classical particles and stable field-like behaviors.

Tier 4 introduces the concept of wavefront propagation as the mechanism by which aggregates move through the substrate. Because aggregates consist of multiple Planck Objects (POs) with internal coordination constraints, they cannot all transition simultaneously. Instead, subsets of POs transition in a staggered sequence, forming coherent wavefronts that propagate the aggregate one unit at a time.

The number and timing of these wavefronts define an aggregate's propagation characteristics. Each wavefront represents a partial advance of the aggregate configuration, and multiple

wavefronts may exist simultaneously. This discrete stepping introduces effective velocity and directionality, constrained by internal coordination costs and bounded strictly below the maximum speed of free PO motion.

Tier 4 formalizes the notion that motion through the substrate is not a smooth translation but a staggered reconfiguration of constituent parts. This allows PMT to model aggregate motion, directional persistence, and internal phase dynamics without invoking continuous trajectories or spacetime curvature.

Tier 5 introduces the concept of z-index, a timing descriptor that captures the sequence and priority of wavefront transitions within an aggregate. While previous tiers describe how aggregates propagate, Tier 5 formalizes the bookkeeping required to represent motion timing across complex, non-simultaneous PO transitions.

The z-index does not describe spatial configuration but temporal sequence: which portions of the aggregate move first, which follow, and how delay between steps affects emergent velocity and inertia. Lower z-indices correspond to earlier-moving segments of an aggregate's structure; higher values mark trailing wavefronts. This sequencing is essential to maintain internal coordination and causal consistency.

Tier 5 also introduces z-index fields as metadata over aggregate structure, enabling formal modeling of phase propagation, reconfiguration timing, and directionally dependent persistence. These fields serve as bridges between Tier 4's raw propagation and Tier 6's dynamic reconfiguration.

Tier 6 introduces the zeta-index, a descriptor of aggregate configuration in terms of spatial structure rather than temporal ordering. While the z-index in Tier 5 tracks when transitions occur, the zeta-index captures which elements of an aggregate participate in each wavefront, effectively describing the "shape" of motion across the substrate.

Multiple zeta configurations may be active within a single aggregate, especially in large or complex systems. These configurations can overlap, interfere, or reinforce one another depending on the internal constraints of the system. Zeta-indices provide a means to map out motion topology across discrete space, offering a granular way to express directional persistence, flexion, or coherence among parts of the aggregate.

Tier 6 also introduces the concept of zeta-superposition, where multiple spatial configurations may be valid at once due to probabilistic or asynchronous transition rules. These superpositions help model aggregate variability and underpin later tiers dealing with statistical mechanics and decoherence.

Tier 7 introduces probabilistic transition mechanics. While previous tiers describe deterministic coordination and propagation rules, Tier 7 acknowledges that large aggregates—especially those with complex or high-zeta configurations—cannot be modeled with strict determinism at scale. Instead, transitions occur with quantifiable probabilities derived from aggregate structure, wavefront sequencing, and environmental context.

This introduces a natural statistical framework for modeling uncertainty, thermal effects, and dynamic reconfiguration. Probabilistic delays, wavefront collisions, and coordination conflicts all contribute to behavior that mimics thermodynamic dispersion and Brownian-like motion. Rather than noise imposed from without, randomness arises internally from high-order structural degeneracy and path entanglement.

Tier 7 thus bridges discrete determinism with emergent stochastic behavior, enabling PMT to describe the conditions under which classically unpredictable behavior arises without abandoning its underlying lattice formalism.

Tier 8 introduces decoherence as the disruption of internal coordination within an aggregate. While earlier tiers model stability and wavefront propagation, Tier 8 addresses how internal structure may partially or entirely break down due to timing failures, environmental perturbation, or conflict between zeta configurations.

Decoherence does not necessarily imply destruction. In PMT, it refers to the loss of statistical persistence in the aggregate's configuration. Depending on severity, this may result in internal reconfiguration, a loss of directional coherence, or the collapse of complex structures into simpler ones.

Tier 8 also introduces thresholds of coherence: criteria by which a structure may retain, regain, or lose its status as a functional aggregate. These thresholds are defined in terms of sustained z-index and zeta-index patterns, permitting a rigorous framework for modeling particle decay, phase shifts, or other transitions in aggregate identity.

Tier 9: Aggregates of Aggregates

Tier 9 introduces a new level of structural emergence wherein previously stable PO aggregates themselves combine to form higher-order composite units. These "aggregates of aggregates" possess their own characteristic identities, interaction rules, and dynamic behaviors that are not reducible to those of their constituent aggregates alone.

Whereas Tier 8 focused on the emergent properties of stable PO groupings—such as momentum, persistence, or coherence, Tier 9 concerns itself with how these structures interrelate, bind, or superpose to form meta-structures. These meta-aggregates may share transition rules, synchronize wavefronts, or give rise to new forms of decoherence that occur not within an individual aggregate, but between aggregates.

Tier 9 marks the point at which the combinatorial space of behaviors explodes, and where the statistical convergence properties noted earlier (e.g., those driven by the law of large numbers) begin to facilitate aggregate classes that exhibit phase-locked dynamics, long-range correlations, or synchronized rest-to-jump cycles. These mechanisms may correspond to the earliest analogues of compound particles or fields.

Tier 9 represents the inception of stable meta-patterns and introduces the possibility of encoding behaviors across multiple layers of structural recursion. It prepares the ground for

the organizational motifs observed in known particles or quasi-particles.

Tier 10 introduces the formal emergence of particle-like entities as stable, re-identifiable configurations of PO aggregates. These structures are no longer mere transient wavefronts or local coherence, but persistent patterns capable of maintaining identity across transitions and interactions. They embody the early analogues of what will eventually correspond to elementary particles in physical models.

Particle encoding in PMT is not arbitrary but constrained by the topological, temporal, and interaction rules established in lower tiers. Each particle-like configuration is characterized by a distinct zeta-index signature, a wavefront topology that remains statistically invariant over many Planck steps. The z-index, meanwhile, captures timing and phase relations critical to the coordination of sub-components within a particle's internal structure.

At this stage, the substrate supports repeatable structures with well-defined probabilistic boundaries, making it possible to define notions of localization, re-identification, and long-range influence. The encoded particle becomes a coherent unit of propagation and interaction, setting the foundation for identity persistence, cross-aggregate communication, and ultimately the interaction schemes of Tier 11.

This tier begins the formal bridge between the purely kinematic structure of PMT and the observable catalog of physical particles.

Tier 11 formalizes interactions between particle-encoded aggregates by defining permissible transition patterns, overlap constraints, and conditional reconfiguration rules. These interactions are local in substrate terms, but manifest as forces or exchanges at higher scales.

At this level, particles are treated not as isolated PO configurations, but as participants in structured exchanges governed by zeta-index compatibility, shared timing via z-index synchrony, and boundary coherence criteria. Interactions are encoded as modifications to the timing or configuration state of one or more particles due to proximity or phase coupling with others.

The core mechanisms in this tier include:

- **Zeta-compatibility**: Interaction requires that the zeta-indices of two aggregates admit at least partial overlap or phase locking.
- **Phase perturbation**: Interaction events result in measurable changes in the internal phase or timing of one or more participants.
- **Aggregate reconfiguration**: Interactions can lead to stable new aggregates or the dissolution of unstable ones.
- **Causal adjacency**: Only aggregates within a defined range, measured in discrete steps and not in meters, can influence each other.

This tier lays the groundwork for modeling quantum field-like behaviors without invoking continuous fields. Instead, interaction is framed as a set of allowed local transformations across PO aggregates, mediated by statistical rules and bounded transition topologies.

Tier 11 thus encodes the primitive analogs of what will eventually be recognized as particle interactions, coupling rules, and fundamental conservation constraints.

Tier 12 ties the entire hierarchy together on cosmological scales. It examines how the discrete Planck-level substrate, through statistical smoothing and the law of large numbers, gives rise to apparently continuous space-time, classical causality, and large-scale structure. Global clock-rate drift of PO rest intervals reproduces cosmic expansion (and a dark-energy–like acceleration term), while Planck-scale jitter seeds density fluctuations that grow into galaxies. Boundary choices—whether an infinite lattice or a finite 3-torus—set the observable topology of the universe, and macroscopic determinism emerges as timing noise is suppressed by $N^{-1/2}$ in large aggregates. Tier 12 therefore completes PMT by demonstrating that classical and relativistic physics are statistical limit cases of a deeper, discrete causal lattice.‴

1. Tier 1: Fundamental Geometry and Planck Motion

The following section establishes the foundational constructs upon which all higher tiers of PMT depend. Tier 1 defines the spatial and temporal primitives of the substrate, introduces the behavior of Planck Objects (POs) as discrete transitions between adjacent lattice cells, and formalizes the rule structure for what will be known as Planck Motion. This level serves as the axiomatic base from which emergent dynamics such as mass, velocity, and energy derive in subsequent tiers.

1.1 The Cubic Lattice

Planck Objects are described as occupying a perfectly regular cubic lattice, with each PO residing in a single, indivisible cubic cell of side length ℓ_p. This lattice is adopted for its pedagogical clarity and ease of modeling discrete motion, but it is not necessarily to be taken as ontologically primary.

The use of a cubic tiling is a deliberate choice for illustrative purposes, though it introduces anisotropy. More isotropic tilings, such as tetrahedral or icosahedral, cannot tile three-dimensional space without gaps. For Tier 1, we accept the anisotropy of the cube to emphasize the discrete character of the model.

For modeling purposes, the substrate lattice is assumed to be infinite in all directions, eliminating edge effects and enabling unrestricted propagation of PO motion.

Statistical Isotropy. Although a single cubic cell is anisotropic, PMT assumes that at scales above $\gtrsim 10^2$–$10^3\,\ell_p$ the lattice orientation varies stochastically. Central–limit averaging then suppresses observable anisotropy as $(\ell_d/L)^{3/2}$, consistent with the standard three–dimensional CLT [2], keeping Lorentz-violation below current bounds except near the Planck scale.

1.2 Discrete Time: The Planck Interval

Time is similarly quantized, though it should be pointed out that at Planck scale, time as human beings commonly understand and experience it may not exist. The human sense of time is theorized to be emergent just as are all other phenomena, advancing in uniform intervals of t_p, the Planck time. No event or interaction occurs in sub-Planck durations. Each PO may perform a unit action per interval: either rest in place or transition to an adjacent cell. This imposes a universal upper bound on temporal resolution, expressed as the Planck Frequency, defined as the reciprocal of the Planck time: $f_p = 1/t_p$ [1].

This value represents the maximum meaningful frequency in PMT and reflects the shortest possible time interval between causally related events.

To characterize large-scale coherence, especially phenomena involving superposition or wave-like behavior, a representational framework is required that can express both phase and probability amplitude. This motivates the use of Hilbert spaces in modeling higher-tier aggregate behaviors within PMT.

Furthermore, even from the perspective of a distant or differently situated observer, no two events—occurring in separate frames or regions—can be temporally resolved to within less than one t_p. All such differences collapse into a single temporal quantum, making simultaneity itself quantized and precluding comparisons of time intervals below this threshold.

Simultaneity Limit. Let e_A and e_B be two events occurring in spatially distinct regions or frames, observed by a third party O. If the measured time difference between them satisfies $|\Delta t| < t_p$, then under PMT's discrete temporal ontology:

$$\Delta t = |t_A - t_B| < t_p \quad \Rightarrow \quad \Delta t \equiv 0.$$

That is, the events are deemed temporally indistinguishable within the limits of the lattice resolution, and no finer ordering can be meaningfully asserted.

This simultaneity quantization yields a finite set of logically permissible detection states from the perspective of observer O:

Event e_A Detected	Event e_B Detected	Resolution Outcome
Yes	Yes	$t_A = t_B$ (quantized simultaneity)
Yes	No	Observer infers e_A occurred first
No	Yes	Observer infers e_B occurred first
No	No	Neither event observed by O

These detection states define the total informational resolution available at the Planck interval, placing an upper bound on temporal discrimination in the substrate.

1.3 Definition of Planck Motion

Planck Motion is defined as the unit action of a PO that instantaneously transitions from one cell to an adjacent one and then rests for a minimum of one t_p. The result is an effective motion at velocity $c = \ell_p/t_p$. Motions involving longer rest intervals for each jump event of a PO yield effective velocities $v < c$.

Importantly, POs may not move diagonally or skip cells. All allowed transitions are to face-adjacent cells only, and each transition is atomic and complete within a single t_p cycle.

The rest state is defined as the absence of a transition during a given t_p cycle. Although no movement occurs, Planck-scale timing advances uniformly, and such rest intervals are critical to determining aggregate velocity.

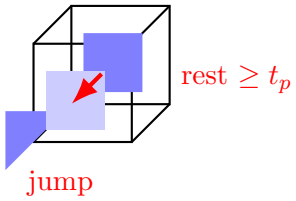

Figure 1: A single Planck Object (PO) executes a unit jump to a face-adjacent cell, then enters its mandatory rest phase of at least one t_p.

1.4 Local Causality and Closure

All permitted actions occur entirely within the closed geometry of the lattice. There is no reference to global coordinates or background spacetime. This constraint ensures strict locality and prohibits classical notions of simultaneity or continuous acceleration.

1.5 The z-index

Although Tier 1 does not employ global timing schemes, later tiers will formalize coordination of rest and motion intervals via a quantity called the *z-index*, representing a PO's timing phase within an aggregate system.

1.6 Completeness Principle

Tier 1 includes a completeness principle: all valid physical actions within PMT can be constructed from sequences of discrete PO transitions and rest states. No higher-level dynamic (e.g., momentum, force) is introduced at this stage.

This establishes a fully contained kinematic substrate, free from classical limit processes, upon which all emergent structure in PMT is hierarchically constructed in levels suggestive of an evolutionary process.

1.7 Self-Organization

PMT posits that Planck Objects are inherently self-organizing. While this assumption is foundational and currently unprovable, it draws heuristic support from numerous examples in nature. Crystalline solids, for instance, exhibit orderly structures arising from simple local rules under appropriate conditions. Self-organization is also observed in biological systems, where complex structures and functions emerge spontaneously from simple constituents.

Such organization stands in contrast to what would be expected from purely random motion, suggesting instead that there exists an intrinsic bias toward local order even at the most fundamental scale.

This principle of spontaneous order is extended downward in PMT to the most fundamental scale, where POs are assumed to aggregate under local transition rules into stable, higher-order configurations. These aggregates form the basis for emergent behaviors observed in higher tiers.

The self-organization postulate draws on precedents in complex systems, where local rules yield emergent order, as seen in cellular automata [3] or dissipative structures [4]. This suggests that Planck Objects, governed by simple transition rules, can form stable aggregates. Future work will formalize these rules to test the assumption (Appendix B).

Although this concept may invite analogies to phenomena such as consciousness or galactic structure, such parallels are speculative and belong to future elaborations beyond Tier 1.

Having defined the discrete substrate and motion rules governing individual Planck Objects,

we now ascend to the second tier, where local interactions among POs give rise to stable aggregates. These structures form the first layer of complexity within PMT, from which emergent behaviors begin to take shape.

1.8 Tier 1 Summary

- **Discrete Substrate:** Space is modeled as a perfectly tiled cubic lattice of side ℓ_p; POs occupy one cell each.
- **Planck Motion Rules:** A PO either *jumps* to a face-adjacent cell or *rests* for at least one Planck tick t_p, enforcing the invariant speed $c = \ell_p/t_p$.
- **Quantized Time and Planck Frequency:** All durations are integer multiples of t_p; the reciprocal $f_p = 1/t_p$[1] is the maximal event rate and forms the harmonic base for higher-tier dynamics.
- **Completeness Principle:** Every admissible physical process is a finite or repeating sequence of PO transitions and rests—no external continuum limits are required.
- **Local Causality:** Actions reference only neighboring cells; simultaneity is quantized ($|\Delta t| < t_p \Rightarrow \Delta t \equiv 0$).
- **Statistical Isotropy:** The cubic lattice is locally anisotropic, but stochastic orientation of 10^2–$10^3\,\ell_p$ domains suppresses anisotropy as $(\ell_d/L)^{3/2}$, retaining empirical Lorentz invariance at macroscopic scales.
- **z-Index Prelude:** Timing phase labels (z) are introduced as the bookkeeping device for future coordination; spatial topology labels (ζ) are deferred to Tier 2.
- **Self-Organization Postulate:** POs possess an intrinsic tendency to form stable, higher-order aggregates—laying the groundwork for all subsequent tiers.

This completes the foundational layer: a fully discrete, locally causal, statistically isotropic substrate from which the rest of PMT's hierarchy emerges.

2. Tier 2: Aggregate Behavior and Coupling

Tier 2 introduces the first-order behaviors of multiple POs acting in coordination. Whereas Tier 1 describes individual transitions, Tier 2 defines the concept of *coupling*—persistent statistical relationships among PO actions—that give rise to the simplest forms of structure and pattern. These aggregates form the foundation for emergent particles, motion coherence, and later field-like behavior.

2.1 Coupling

Coupling is defined as a statistically persistent correlation in the behavior of two or more Planck Objects. A coupled group of POs exhibits interdependent timing, directional preference, or positional correlation not attributable to pure randomness. It is not a spatial or mechanical constraint, but a temporal coordination that endures across many Planck intervals.

2.2 Coupling Mechanisms

Coupling may arise from:

- **Local transition rules:** Neighbor-dependent rules can promote coordinated behavior among adjacent POs.
- **Shared z-index alignment:** Common timing phases allow synchronous or staggered coupling.
- **Emergent locking:** Stochastic patterns that persist under local feedback can stabilize into sustained aggregates.
- **Geometry and boundary conditions:** Lattice constraints and surrounding aggregates may promote locally stable couplings.

These mechanisms are not imposed from above but emerge naturally under the transition dynamics of the substrate.

2.3 Staggered Coordination

Coupled POs are often staggered in their transition phases. Rather than moving simultaneously, members of the aggregate transition in a sequenced pattern, separated by discrete time offsets. This staggering prevents collision (double occupancy) and introduces temporal structure within the aggregate.

The result is an effective group velocity that is less than c and a kind of distributed internal clocking, which forms the foundation of inertial properties.

2.4 Wavefront Propagation

The staggered transitions of a coupled PO group produce a wavefront—the advancing edge of active motion. The aggregate moves not as a block but as a sequence of local transitions,

like a ripple through the substrate.

This structure permits the modeling of directional motion, coherence, and internal timing patterns consistent with emergent particle behaviors. It is also the basis for describing group velocity.

2.5 Statistical Persistence

For coupling to yield meaningful aggregates, the correlated pattern must persist statistically over time. Aggregates are not rigid structures but probabilistic entities: their internal configuration remains consistent with high probability across many Planck intervals.

This persistence allows aggregates to maintain identity and coherence even as individual POs transition or rest. It is a threshold criterion for distinguishing signal from noise.

Decoherence. When the phase alignment or coupling integrity among constituent POs of an aggregate is disrupted beyond a critical threshold, the system may undergo *decoherence*. In PMT, decoherence does not necessarily imply destruction of the aggregate but can involve a structural reconfiguration or partial disintegration, resulting in loss of coherence-dependent behaviors such as directed propagation or interference. This sets a functional boundary on the persistence of coherent aggregates in fluctuating environments, and will be examined further in higher tiers dealing with interaction and thermodynamics.

2.6 Decoherence

Decoherence in PMT is the loss of internal phase alignment, coherence, or structural integrity within a PO aggregate, resulting in the collapse or transition of the aggregate to a different behavioral regime. Because aggregate coherence depends on both temporal coordination (z-index) and spatial topography (zeta-index), decoherence can result from disruptions to either or both components of what is collectively termed the *z-complex*.

This z-complex characterizes both the synchronization patterns of PO transitions (via z-index) and the coupling geometry that defines the aggregate's structural stability (via zeta-index). A breakdown in this coordination — whether due to external disturbance, internal instability, or quantum interaction — causes the object to become unstable or transition to a new configuration.

Decoherence, then, is not merely a loss of quantum superposition but a structural and organizational shift in the configuration of a PO aggregate. Depending on the severity, decoherence may:

- alter the object's effective mass, frequency profile, or momentum
- partially degrade coherence without destroying the full aggregate (e.g., a vibrational mode decaying)
- cause fragmentation into lower-tier substructures

Because PMT models all higher-order behaviors as arising from coupling regimes within discrete structures, decoherence represents the point at which these couplings fail to maintain system-wide identity. This is a structural collapse, not simply a probabilistic shift.

The role of decoherence in measurement or environmental interaction remains a key avenue for future development, particularly in how Planck-scale disruptions scale up to classical observational effects.

2.7 Resolution of Wave–Particle Duality

PMT resolves the classical wave–particle duality by modeling both behaviors as emergent traits of coupled PO aggregates, varying with configuration, coherence, and scale. Rather than treating "wave" and "particle" as fundamentally distinct ontologies, PMT frames them as two regimes on a discretely gradated behavioral spectrum that appears continuous at large scales.

The apparent mode of behavior—wave-like or particle-like—depends largely on how the aggregate is consumed by the measurement apparatus. Some configurations will collapse in a particle-like manner, yielding discrete location data; others will exhibit interference, diffraction, or resonance patterns, revealing wave-like behavior.

At this level, PMT introduces the notion of the zeta-index, denoted by ζ, representing the internal topography or dynamic configuration profile of a PO aggregate.

Zeta-index Definition. Let ζ denote the configuration descriptor of a PO aggregate, encoding both spatial structure and coupling topology. Unlike the z-index, which tracks temporal phase per PO, ζ captures the emergent, often dynamic, organization of multi-PO systems.

It should also be noted that an aggregate object may manifest both wave- and particle-nature simultaneously, depending on the zeta-index profile. In PMT, an aggregate could be of a spheroidal layout, tightly coupled. An aggregate might also have all manner of undulations like ripples on the surface of calm water after having thrown in a pebble. The discrete and composite nature of aggregates provides a practically endless list of possible configurations.

The zeta-index for an aggregate may describe highly intricate internal architectures. For example, imagine an aggregate whose core is a tightly coupled spheroid, exhibiting great

internal coherence and behaving in a highly localized fashion. Radiating outward, the structure might feature concentric shells or rings—perhaps forming a disk- or saucer-like profile—composed of wave-like undulations or loosely coupled substructures. These external formations could span volumes significantly larger than the core and may vary dynamically with time or environment. Localized differences in coupling schemes across such a structure would yield a rich and multifaceted zeta topology, potentially encoding a broad array of emergent traits even at the scale of known fundamental particles.

Structural Role of the Zeta-index. An open question in PMT is whether the ζ-index is merely a descriptive topographic label or a structural substrate composed of POs that causally dictates the aggregate's behavior. If ζ arises from persistent PO configurations—acting analogously to DNA in biological systems—then it may function as a self-organizing template that governs coupling, phase coherence, and wavefront architecture.

Such a view implies that aggregates possess internal regulatory structures that determine how motion, interaction, and decoherence unfold over time. The ζ-index would then not simply describe emergent form but participate actively in its preservation and transformation.

2.8 The Z-Complex

As introduced earlier, PMT employs two distinct but complementary indices to describe timing and structural topography within PO aggregates: the *z-index* and the *zeta-index*. Together, these form what we now call the **z-complex**.

The **z-index** refers to the timing phase of a given Planck Object or substructure within an aggregate. It determines when a PO is permitted to transition, and how its motion relates to other POs in a coupled group. Aggregates with coordinated z-indices exhibit coherence, enabling effective propagation of structure across the lattice in the form of composite motion.

The **zeta-index**, by contrast, describes the geometric and topological wavefront structure of an aggregate. It encodes which parts of the aggregate are active at any given interval, and captures spatial configurations such as internal nodes, shells, or radiating fronts.

These two indices operate jointly: z controls *when*, and zeta controls *what* and *where*. Together, they define the dynamic behavior of complex aggregates, including apparent wave or particle behavior depending on how the structure interacts with measuring systems.

It should also be noted that an aggregate may exhibit simultaneous wave- and particle-like behavior, depending on its zeta-index profile. In PMT, a structure might consist of a tightly coupled spheroidal core with concentric, extended undulating layers that behave as standing or propagating wavefronts. The z-complex governs how such internal and external structures cohere or de-cohere under interaction.

A particularly provocative conjecture is that the zeta-index itself may be more than a descriptive overlay; it may reflect an internal structure of POs that function analogously to a physical genome, encoding aggregate form and function. This would position the z-complex not only as a behavioral index but as a generative template.

As Tier 2 closes, the z-complex provides the critical framework for understanding emergent identity and behavioral stability across scales, bridging stochastic Planck-level action with recognizable physical structures.

2.9 Structural Complexity

PMT holds that aggregate entities—composed of coupled Planck Objects—can possess deeply layered internal configurations, resulting in structural complexity far beyond what is typically associated with quantum particles.

One measure of this complexity arises from the nature and arrangement of zeta-index profiles. The zeta-index describes the wavefront and spatial topography of an aggregate, and it may do so across multiple, simultaneous configurations. These layered arrangements give rise to two key notions: *Zeta Multiplicity* and *Behavioral Overlap*.

Zeta Multiplicity. Zeta Multiplicity refers to the coexistence of multiple distinct zeta-index configurations within a single aggregate. These configurations may represent separate propagation modes, nested wavefronts, or overlapping coupling regimes. Each configuration contributes to the aggregate's overall behavior and determines its interaction patterns with external systems. The more zeta modes present, the richer the aggregate's dynamic repertoire.

Behavioral Overlap. Behavioral Overlap occurs when distinct physical behaviors—traditionally considered mutually exclusive—manifest simultaneously within different sub-regions or structural layers of the same aggregate. For instance, a PO aggregate may exhibit both wave-like propagation and localized, particle-like coherence, depending on the coupling density and zeta-pattern in each region. This phenomenon offers a possible explanation for hybrid behaviors observed in certain quantum systems, without invoking collapse or superposition in the classical sense.

Together, Zeta Multiplicity and Behavioral Overlap help explain how even the smallest quantum entities may encode vast behavioral and structural variation, pointing toward a higher-order architecture encoded at the Planck scale.

2.10 Tier 2 Summary

Tier 2 expands upon the discrete motion rules of Tier 1 by introducing coupling behaviors among Planck Objects and the aggregate-level dynamics that emerge from these interactions. The key insights of this tier include:

- **Coupling and Coupling Mechanisms:** Aggregates form through stable, synchronized interactions between POs. These interactions are governed by transition rules that permit synchronization of rest and motion cycles, forming durable composite structures.
- **Staggered Coordination:** The coordination of PO actions need not be simultaneous but may follow staggered, rule-governed sequences. This property permits the formation of persistent, propagating configurations.
- **Wavefront Propagation:** Rather than moving collectively, aggregates propagate through tiered advancement of constituent POs, giving rise to coherent wavefronts, foundational to later notions of fields and particles.
- **Statistical Persistence and Decoherence:** Aggregate stability arises probabilistically and can be disrupted by external perturbation or internal disarray. Decoherence occurs when the coherence of the system degrades beyond the ability to self-sustain its zeta-structure.
- **Resolution of Wave–Particle Duality:** PMT re-frames wave and particle behaviors as emergent regimes of aggregate configuration. These behaviors manifest contextually, often simultaneously, depending on how aggregates interact with measurement apparatus.
- **The Z-Complex:** The z-index governs the timing of PO transitions; the zeta-index governs the topographic and coupling profile. Together, they form a higher-order construct—the z-complex—that defines the behavioral constraints of aggregates.
- **Structural Complexity:** Aggregates may exhibit multiple simultaneous zeta-configurations, resulting in hybrid behaviors and rich internal architectures. This tier introduces the concepts of zeta multiplicity and behavioral overlap, laying the groundwork for emergent properties in higher tiers.

Together, these elements provide a bridge from fundamental lattice motion to increasingly complex systems of behavior, positioning Tier 2 as the substrate-level origin of observable particle structure, probabilistic behavior, and quantum-classical transition.

3. Tier 3: Emergence of Mass, Energy, and Momentum

This tier addresses the emergence of mass, energy, and momentum from lower-tier behaviors of Planck Objects (POs), governed by timing constraints, coordination structures, and coupling persistence. Unlike classical theories in which mass and energy are fundamental attributes, PMT treats them as consequences of substrate-level dynamics.

3.1 Effective Mass from Coordination Delay

In PMT, mass is modeled not as an intrinsic property, but as an emergent behavior of an aggregate's internal coordination delays. When Planck Objects within an aggregate cannot synchronize transitions due to coupling constraints, the aggregate's group velocity becomes limited. This deviation from the speed of light corresponds to effective mass. Thus, mass is inversely related to the freedom of propagation.

3.2 Inertial Response and Timing Lock

The concept of inertia emerges from the temporal locking of PO transitions. In tightly coupled systems, coordinated transitions become staggered across multiple Planck time intervals. Any attempt to change the velocity of such a system requires re-coordination of all internal timing states. This gives rise to the phenomenon of resistance to acceleration, which is classically interpreted as inertia.

3.3 Energy as Aggregated Transition Effort

Energy in PMT is the total count of successful transition attempts within a given z-index frame. A PO aggregate whose members are frequently transitioning or maintaining coherence across a spatially extended structure embodies higher energy. Energy thus maps to cumulative PO activity per unit z-index, not to a continuous variable.

3.4 Momentum as Directional Transition Bias

Momentum arises from statistical asymmetry in the directionality of PO transitions. Aggregates exhibiting a sustained directional bias—maintained across coherent timing phases—are said to carry momentum. This is not a stored quantity but an emergent consequence of organized propagation in a preferred direction.

3.5 Mass-Energy Equivalence Reinterpreted

PMT accommodates a reinterpretation of the mass-energy relation $E = mc^2$. Since mass and energy both arise from transition dynamics—mass from temporal delay, energy from total activity—their interchangeability reflects their shared substrate basis. What appears as "conversion" is actually a shift in the aggregate's transition mode.

3.6 Relativistic Limits Without Continuity

All Tier 3 behaviors preserve relativistic constraints without invoking continuous spacetime. The effective upper bound $c = \ell_p/t_p$ is enforced by the unit behavior of Planck Motion. No PO or aggregate can exceed this propagation rate due to discrete timing and transition limits.

3.7 Inverted Fourier Cascade

The fundamental Planck frequency is

$$f_p \;=\; \frac{1}{t_p}.$$

When an aggregate requires N_{rest} additional rest ticks between jumps, its cycle frequency becomes the integer sub-harmonic

$$f_N \;=\; \frac{f_p}{N_{\text{rest}} + 1}.$$

Larger, slower aggregates therefore populate a *downward* (inverted) harmonic ladder of f_p. If the distribution of N_{rest} across all aggregates is broad, the power spectrum of PO activity approaches a $1/f$ form frequently observed in complex systems. [5].

Energy scaling. Tier 3 defines energy as cumulative transition effort; for a single harmonic mode

$$E_N \;=\; \hbar_{\text{eff}}\, f_N, \qquad \hbar_{\text{eff}} \;=\; \frac{\ell_p^2 c^3}{G}\,.$$

Thus energy and mass both diminish with increasing harmonic index, linking low-frequency modes to high effective inertia.

Hierarchy of modes. Because every higher-tier aggregate inherits its timing from constituent modes, the entire twelve-tier hierarchy can be viewed as a nested, inverted Fourier cascade from f_p down to macroscopic frequencies.

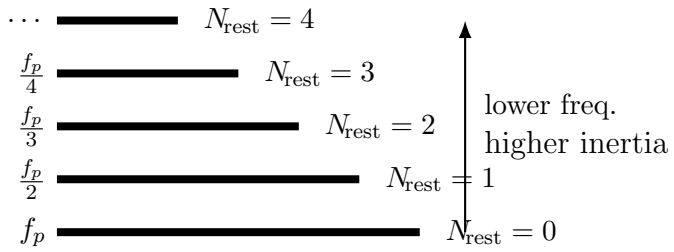

Figure 2: The inverted Fourier cascade: each extra rest–tick N_{rest} lowers the aggregate's cycle frequency to $f_p/(N_{\text{rest}} + 1)$, building the harmonic ladder discussed in §3.7.

3.8 Tier 3 Summary

- Mass arises from coordination delay; inertia from timing-lock resistance.
- Energy equals aggregate transition density; momentum is directional bias.
- A discrete Lorentz factor recovers time dilation and length contraction.
- An inverted Fourier cascade maps rest-interval counts to sub-harmonic frequencies, unifying mass–energy scaling with PO timing.

4. Tier 4: Field-Like Interaction and Signal Propagation

Tier 4 shows how PO aggregates influence one another across the lattice without invoking continuous fields. All effects arise from discrete, local timing perturbations that propagate no faster than $c = \ell_p/t_p$.

4.1 Interaction Fronts

When two aggregates enter causal range (face-adjacent or separated by a thin layer of empty cells), a *coordination front* is emitted:

1. Boundary POs in the source shift phase by $\Delta z = \pm 1$.
2. That shift propagates cell-by-cell as a staggered sequence of Planck-motion steps.
3. Upon arrival, the target's boundary POs undergo a compensating timing shift, altering its internal z-schedule or local ζ-profile.

These fronts play the role traditionally assigned to boson exchange.

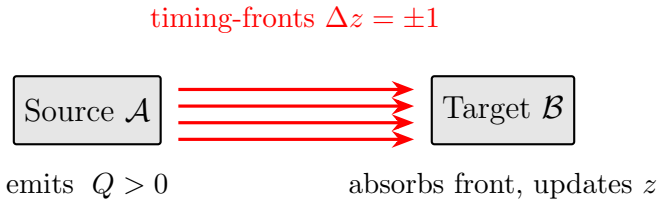

Figure 3: Series of coordination fronts (red arrows) emitted by source aggregate $\mathcal{A}$ and absorbed by target $\mathcal{B}$. Each front carries a discrete phase shift that mediates the Tier 4 interaction.

4.2 Charge-Like Asymmetry

Define a *coupling polarity*

$$Q \;=\; \sum_{i \in \partial \mathrm{Agg}} \left(z_i^{\mathrm{out}} - z_i^{\mathrm{in}} \right),$$

the signed excess of outward over inward phase shifts per cycle. Aggregates with $Q \neq 0$ emit or absorb fronts asymmetrically and therefore mimic electric-charge behaviour: opposite polarities synchronize (attract), identical polarities stay out of phase (repel). Geometric dilution of front density yields an emergent $1/r^2$ law, matching Coulomb fall-off [6].

4.3 Discrete Gauge Freedom

Because only *relative* timing matters, every PO in an aggregate may be advanced by the same integer k without physical effect:

$$z_i \;\mapsto\; z_i + k, \qquad k \in \mathbb{Z}.$$

This lattice redundancy is a discrete analogue of gauge freedom; interaction laws remain invariant under global z-shifts.

4.4 Signal Propagation and Information Speed

A sequence of fronts with variable spacing encodes information. The fastest signal speed equals c; slower signaling is achieved by padding rest cycles. Error-free communication requires the coherence length λ_{coh} to exceed the decoherence mean-free-path $\ell_{\mathrm{dec}} \approx (p_{\mathrm{dec}})^{-1} \ell_p$, where p_{dec} is the local decoherence probability per cell.

4.5 Effective Potentials

Repeated front exchange generates an averaged *coordination budget* cost vs. distance:

$$V(r) \;=\; \kappa\,\frac{Q_1 Q_2}{r^2}\,[1 + O(r^{-1})],$$

with κ fixed by lattice geometry and decoherence rate. Aggregates with $Q = 0$ interact via higher-order (multi-polar) front patterns, reproducing van-der-Waals-like attraction at short separation.

4.6 Conservation via Front Book-Keeping

Every emitted front decrements the source's local timing budget and, after transit delay, increments the target's. Because budgets are discrete and fronts propagate without loss, total "coupling charge" and total timing budget are conserved, supplying a lattice foundation for energy- and momentum-like conservation laws.

4.7 Tier 4 Summary

Tier 4 replaces classical fields with propagating coordination fronts:

- Local interaction is a timing perturbation transmitted cell-by-cell.
- Persistent phase asymmetry (Q) yields charge-like forces with $1/r^2$ behavior.
- Global integer shifts in z constitute a discrete gauge symmetry.
- Information moves at or below c via front trains.
- Conservation laws arise from integer book-keeping of timing budgets.

These results prepare Tier 5, where cumulative timing delays produce relativistic effects such as time dilation and Lorentz-like contraction.

5. Tier 5: Relativistic Behavior from Timing Delays

Tier 5 demonstrates how special-relativistic effects arise in PMT without continuous space-time. Finite propagation speed and internal timing budgets of PO aggregates naturally reproduce Lorentz-like kinematics.

5.1 Kinematic Delay and Effective Velocity

A single PO alternates *jump* and *rest*. Let n_{rest} be the number of t_p cycles spent resting after each jump. The average velocity is

$$v \;=\; \frac{\ell_p}{(n_{\text{rest}}+1)\,t_p}.$$

Aggregates inherit additional coordination delays Δn from internal coupling, so their group velocity is

$$v_{\text{agg}} \;=\; \frac{\ell_p}{\big(n_{\text{rest}}+\Delta n+1\big)\,t_p}, \qquad v_{\text{agg}} < c.$$

5.2 Discrete Lorentz Factor

Define

$$\gamma \;=\; \frac{n_{\text{rest}}+\Delta n+1}{n_{\text{rest}}+1} \;=\; \frac{c}{v_{\text{agg}}}.$$

For large aggregates $\Delta n \gg n_{\text{rest}}$, we may write $\gamma \approx 1/\sqrt{1-v_{\text{agg}}^2/c^2}$, matching the continuous Lorentz factor to leading order.

5.3 Time Dilation

An internal clock in the aggregate marks one "tick" per full cycle of its local z-schedule. An external observer measures a dilated interval:

$$\Delta t_{\text{obs}} \;=\; \gamma\,\Delta t_{\text{proper}} \;=\; \frac{n_{\text{rest}}+\Delta n+1}{n_{\text{rest}}+1}\,\Delta t_{\text{proper}}.$$

Thus timing delays inside the aggregate manifest exactly as relativistic time dilation.

5.4 Length Contraction

Because propagation occurs via staggered wavefronts, the leading and trailing edges of an aggregate cannot jump simultaneously. The longitudinal separation in the lab frame is compressed by γ^{-1}, giving

$$L_{\parallel} \;=\; \frac{L_0}{\gamma},$$

while transverse dimensions remain unchanged, reproducing Lorentz–FitzGerald contraction.

5.5 Relativity of Simultaneity

Tier 1's simultaneity limit ($|\Delta t| < t_p \Rightarrow \Delta t \equiv 0$) applies only within a single rest-frame lattice region. Aggregates moving at different v carry distinct z-schedules, so events simultaneous for one may differ by multiples of t_p for another—yielding the discrete analogue of relativity of simultaneity.

5.6 Energy–Momentum Relation

Using Tier 3 definitions (E as transition density, p as directional bias) and the discrete γ above:

$$E^2 - (pc)^2 \;=\; (\gamma m_0 c^2)^2 - (\gamma m_0 v_{\text{agg}} c)^2 \;=\; m_0^2 c^4,$$

where m_0 is the effective rest-mass from coordination inertia. The familiar continuous formula follows.

5.7 Summary of Tier 5

- Internal rest-to-jump ratios impose aggregate velocities $v < c$.
- Additional coordination delay Δn supplies a discrete Lorentz factor γ.
- Time dilation, length contraction, and relativity of simultaneity emerge directly from PO timing budgets.
- The standard energy–momentum relation follows without a continuous metric.

Tier 5 thus recovers special relativity as a large-scale approximation of discrete Planck-level timing, preparing for Tier 6, where stochastic variations introduce thermodynamic and quantum-statistical phenomena.

Future Work: Lattice Isotropy

Although our Tier-1 substrate is a fixed cubic lattice, a fully Lorentz-invariant phenomenology demands that residual anisotropy be driven below current experimental bounds ($\Delta c/c \lesssim 10^{-22}$ [7] from modern Michelson–Morley tests). A forthcoming companion paper will analyze three candidate mechanisms:

1. **Domain Averaging:** stochastic orientation patches of size $\ell_d \sim 10^2$–$10^3\,\ell_p$ whose central-limit suppression scales as $(\ell_d/L)^{3/2}$.

2. **Quasi-crystalline Embeddings:** higher-rank tilings that approximate isotropy via non-periodic angular spectra.
3. **Dynamic Orientation Fluctuations:** slow re-orientations of local cells that time-average directional biases.

Quantitative convergence rates and observational signatures will be presented there. For the present work we restrict attention to length-scales where central-limit averaging renders the lattice effectively isotropic.

6. Tier 6: Probabilistic Dynamics and Thermodynamic Emergence

Tier 6 introduces controlled stochasticity into Planck-Motion Theory. Random variation in PO transition timing, coupling strength, and zeta–configuration drives macroscopic phenomena usually attributed to statistical mechanics and quantum probability.

6.1 Sources of Stochasticity

1. **Timing Jitter.** Each PO's rest interval may deviate by ± 1 Planck tick with probability p_{jit}.
2. **Coupling Fluctuation.** Temporary weakening/strengthening of a bond between adjacent POs occurs with probability p_{coup}.
3. **Environmental Noise.** Interaction fronts from distant aggregates introduce phase noise of amplitude δz.

All random events are local and memory-less; long-range correlations arise only by propagation through the lattice.

6.2 Master Equation for Aggregate Populations

Define $P(\mathcal{Z}, t)$ as the probability of an aggregate possessing z-complex $\mathcal{Z} = (z, \zeta)$ at step t. Transition rates $W(\mathcal{Z} \to \mathcal{Z}')$ come from the Tier 1–Tier 5 rules plus the stochastic sources above, yielding

$$\frac{dP(\mathcal{Z}, t)}{dt} \;=\; \sum_{\mathcal{Z}'} \Big[W(\mathcal{Z}' \to \mathcal{Z}) P(\mathcal{Z}', t) - W(\mathcal{Z} \to \mathcal{Z}') P(\mathcal{Z}, t) \Big].$$

In the continuum limit of large aggregates this reduces to a Fokker–Planck-type equation.

6.3 Temperature as Transition Dispersion

Let σ_z^2 be the variance of rest-interval fluctuations inside an aggregate. Define an effective temperature

$$k_B T \;\equiv\; \alpha\, \sigma_z^2,$$

with α a geometry constant. Higher jitter thus maps to higher thermodynamic temperature, linking kinetic theory to PO timing noise.

6.4 Entropy and Information Loss

Entropy S of an aggregate ensemble is

$$S \;=\; -\sum_{\mathcal{Z}} P(\mathcal{Z}) \ln P(\mathcal{Z}),$$

rising whenever timing jitter or coupling fluctuation broadens the distribution. Tier 1 closure guarantees Liouville-like conservation of total phase-space volume; entropy growth reflects coarse-graining over untracked micro-states.

6.5 Quantum-Statistical Analogs

For aggregates with large Zeta Multiplicity, phase-coherent subsets evolve under a Lindblad-type map:

$$\rho_{t+1} \;=\; \sum_k L_k\, \rho_t\, L_k^\dagger, \qquad \sum_k L_k^\dagger L_k = I.$$

Here ρ is a reduced density operator over zeta-modes; L_k encode random decoherence events. Schrödinger-like evolution appears when noise terms vanish.

6.6 Fluctuation–Dissipation in Discrete Form

Response of an observable O to a small phase perturbation δz satisfies

$$\langle O(t)\, O(0)\rangle \;-\; \langle O\rangle^2 \;=\; \frac{k_B T}{\gamma} \frac{\partial}{\partial t} \langle O\rangle$$

with γ an aggregate-specific damping factor determined by p_{jit} and p_{coup}.

6.7 Tier 6 Summary

- Local jitter and coupling noise introduce probabilistic dynamics while preserving lattice causality.
- A master-equation framework links micro rules to ensemble evolution and entropy.
- Effective temperature, entropy, and fluctuation–dissipation emerge from timing dispersion.
- Quantum-statistical formalisms (density matrices, Lindblad maps) arise naturally for high-multiplicity zeta states.

Tier 6 thereby unifies thermodynamic and quantum-statistical behavior within PMT's discrete lattice, setting the stage for Tier 7, where measurement, collapse, and macroscopic decoherence are treated explicitly.

7. Tier 7: Measurement, Collapse, and Macroscopic Decoherence

Tier 7 explains how definite outcomes arise when a PO aggregate (the *system*) interacts with a much larger aggregate (the *apparatus*) whose z-complex is already well outside the coherence scale of the system.

7.1 Observer Coupling as Aggregate–Aggregate Interaction

A measurement device is modeled as a high-entropy PO aggregate A with a vast phase-space of zeta-configurations. When the system aggregate S contacts A, their boundary POs exchange coordination fronts exactly as in Tier 4, but A's enormous timing budget absorbs the perturbation irreversibly, imprinting S's state into a stable sub-structure of A.

7.2 Collapse as Zeta-Pruning

Prior to contact, S may carry a *zeta multiplicity*—several coexistent spatial modes. Interaction selects a single mode that satisfies the local coupling constraints of A; all other modes de-cohere within $t_{\text{dec}} \sim O(10^2 - 10^3)\, t_p$. This deterministic pruning appears probabilistic because the micro-state of A is unknowable; the selection probability equals the relative timing budget available to each zeta mode, yielding the Born-rule weight

$$P(\zeta_i) = \frac{B_i}{\sum_j B_j},$$

where B_i is the coordination budget matched between mode ζ_i and apparatus sub-structure A_i.

7.3 Emergence of Classical Pointer States

The surviving joint aggregate $S \cup A_i$ enters a low-entropy, high-statistical-persistence configuration whose macroscopic parameters (e.g. pointer deflection) are robust under further PO-level noise. Classical definiteness is therefore an *attractor* in z-complex space, not an axiom.

7.4 Macroscopic Decoherence Rate

For a macroscopic device of mass M and surface area A_s:

$$\Gamma_{\text{dec}} \;\approx\; \frac{A_s}{\ell_p^2}\, p_{\text{front}}\, v_{\text{front}},$$

where p_{front} is the average probability per cell of an incoming timing front and $v_{\text{front}} \leq c$. Even minuscule p_{front} yields sub-Planck decoherence times for kilogram-scale objects.

7.5 Entanglement as Shared Timing Graph

If two distant aggregates share a common subset of synchronized POs (created, e.g., in a Tier 4 interaction), their z-complex includes a *timing graph* spanning both locations. Measurement at one end prunes the shared graph, instantaneously selecting a compatible mode at the other end. No super-luminal signaling occurs, because changes remain locked in the interior timing graph until a local interaction extracts them.

7.6 Born Rule as Budget Fraction

Let B_{tot} be the total timing budget in the joint $S{+}A$ boundary region; each zeta mode ζ_i occupies B_i budget units. Because fronts conserve budget (Tier 4), selection probability is proportional to B_i. For two-mode superpositions this reproduces the cosine-squared interference pattern of a two-slit experiment when apparatus phases are scanned.

7.7 Tier 7 Summary

- Measurement is an aggregate–aggregate interaction that deterministically prunes zeta multiplicity.

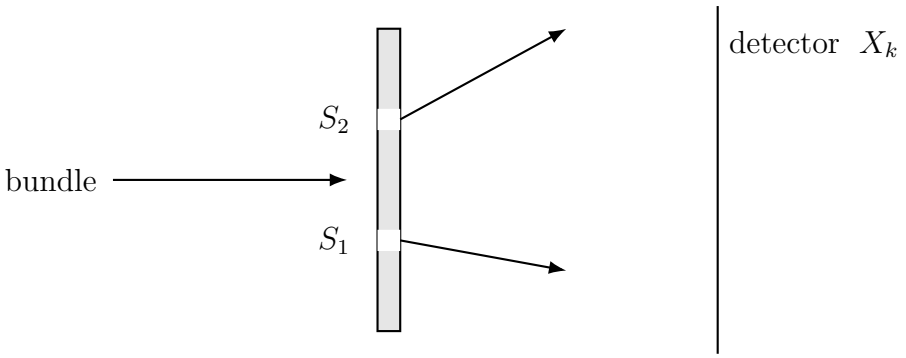

Figure 4: Timing-bundle two-slit schematic used in the Tier 6 example calculation.

- Collapse probabilities arise from discrete coordination-budget ratios, yielding the Born rule without postulating randomness.
- Classical pointer states are attractors in z-complex space—robust, low-entropy configurations of the measuring apparatus.
- Macroscopic decoherence times are Planck-short, explaining why classicality dominates at human scales.
- Entanglement reflects a shared timing graph; "instantaneous" correlations do not violate causality.

Tier 7 thus bridges microscopic stochasticity (Tier 6) and macroscopic definiteness, preparing Tier 8, where large ensembles of aggregates give rise to effective field-like phenomena.

8. Tier 8: Field Analogues and Long-Range Correlation

Tier 8 shows how large ensembles of PO aggregates produce continuum-like "fields" without invoking an underlying continuous substrate. Field behaviour arises as the statistical envelope of many interaction fronts (Tier 4) and timing-budget exchanges (Tier 5–7) distributed over macroscopic regions.

8.1 Ensemble Superstructures

Consider a spatial region containing $\mathcal{N} \gg 1$ aggregates. Each aggregate emits/absorbs coordination fronts with polarity Q_i. The net front density at lattice site $\mathbf{r}$ and discrete time t is

$$\Phi(\mathbf{r}, t) \;=\; \sum_{i=1}^{\mathcal{N}} \frac{Q_i}{|\mathbf{r} - \mathbf{R}_i(t)|^2},$$

smoothed over many cells. Φ behaves as a classical scalar potential in the continuum limit.

8.2 Effective Continuous Fields

Define the coarse-grained field

$$\mathbf{E}(\mathbf{r}, t) \;=\; -\nabla_\ell \Phi(\mathbf{r}, t),$$

where ∇_ℓ is the discrete lattice gradient. For wavelengths $\lambda \gg \ell_p$ the difference quotient reproduces the standard gradient, giving rise to an inverse-square "electric" field.

8.3 Electromagnetic Analogue

If alternating polarity aggregates circulate timing fronts along a closed lattice loop, the resulting front flow mimics a magnetic flux. A time-varying Φ induces an orthogonal circulation of coordination budgets, giving a discrete version of Faraday's law:

$$\nabla_\ell \times \mathbf{E} \;=\; -\Delta_t \mathbf{B},$$

with all derivatives interpreted on the lattice.

8.4 Curvature and Gravitational Analogue

Aggregates with large effective mass (Tier 3) locally slow PO transition rates in nearby cells, stretching the effective tick interval from t_p to $t_p(1 + \delta)$. A spatially varying $\delta(\mathbf{r})$ produces geodesic-like PO paths bending toward slower-clock regions, reproducing classical gravitational deflection.

8.5 Gauge-Redundancy Refinement

Global addition of an integer phase k to all z-indices in a region shifts Φ by a constant; $\mathbf{E}$ and physical observables remain invariant. Local phase shifts that vary slowly over many cells correspond to lattice $U(1)$ gauge transformations.

8.6 Field Quantization Outlook

Individual coordination fronts behave as discrete quanta; coherent superpositions of many fronts yield the classical field Φ. Tier 9 will show how creation/annihilation of front bundles maps onto photon-like and gluon-like excitations.

8.7 Tier 8 Summary

- Macroscopic fields arise as coarse-grained densities of timing fronts and budget flows.
- Inverse-square electric-like and magnetic-like laws emerge for wavelengths $\lambda \gg \ell_p$.
- Mass slows local clock rates, yielding a curvature analogue consistent with gravitational attraction.
- Discrete gauge freedom reproduces continuous $U(1)$ invariance at large scales.
- Field quanta correspond to coherent bundles of coordination fronts, setting up Tier 9's treatment of particle-like excitations of the field envelope.

9. Tier 9: Particle Excitations of Emergent Fields

Tier 8 showed how coarse-grained densities of Planck-Object (PO) coordination fronts behave as classical fields. Tier 9 now identifies *quantized bundles of those fronts*—stable, re-identifiable PO aggregates riding on the field envelope—as particle-like excitations.

9.1 Front Bundles as Field Quanta

A *front bundle* is a phase-locked packet of N_f coordination fronts whose relative timing and polarity remain fixed over many lattice steps. The bundle propagates at c (if strictly phase-locked) or at sub-luminal speed if additional rest ticks are inserted.

Photon Analogue. For the electromagnetic-like field of Tier 8, the lightest bundle ($N_f = 1$, single polarity flip) corresponds to a photon analogue. Higher-energy bundles carry proportionally larger N_f and map to multiple-photon states.

9.2 Charge–Flux Quantization

Because timing budgets are integer-valued, the net polarity flux through any closed surface is quantized:

$$\oint \mathbf{E}\cdot d\mathbf{S} \;=\; Q_{\text{enc}} \;=\; n\,Q_0, \qquad n \in \mathbb{Z},$$

with Q_0 the unit coupling polarity (Tier 4). Bundles therefore carry discrete charge quanta, reproducing charge quantization without fundamental point charges.

9.3 Massive Field Quanta

Bundles whose internal Zeta profiles include rest delays $\Delta n > 0$ propagate sub-luminally and manifest an effective mass $m_{\text{bundle}} = \gamma^{-1} N_f Q_0 \ell_p / t_p$, where γ is the Lorentz factor from Tier 5. Such bundles model massive vector bosons or, with appropriate self-coupling, hadron-like states.

9.4 Fermion-Like Aggregates

A front bundle whose Zeta topology contains an unpaired half-cycle twist (discrete analog of a 2π phase deficit) cannot superpose with another identical bundle without a timing conflict. This exclusion reproduces effective Fermi statistics: only one such mode can occupy a given timing state. The lattice therefore supports fermion-like excitations distinct from bosonic front bundles.

9.5 Composite Structures

Bundles may bind via residual timing attractions (multi-polar front exchange). Two photons of opposite polarity looping around one another form a neutral composite with effective spin-2 behavior—an emergent graviton analogue. Similar binding rules at higher multiplicities yield hadron-like spectra, with confinement arising from the energy cost of isolating individual polarity flux tubes.

9.6 Scattering and Interaction Vertices

When bundles overlap, coordination fronts can re-route, conserving total timing budget and polarity. At coarse-grained scales these interactions map onto familiar Feynman-diagram vertices:

- Photon–electron scattering = polarity-bundle deflection by a fermion twist.
- Pair creation = front-bundle bifurcation under high Φ density.
- Weak-like interactions = exchange of massive timing-delay bundles.

9.7 Tier 9 Summary

- Field quanta are phase-locked bundles of coordination fronts.

- Integer timing budgets enforce charge and flux quantization.
- Sub-luminal bundles acquire effective mass via internal rest delays.
- Half-cycle timing twists yield fermion-like exclusion behavior.
- Composite bundles and front re-routing reproduce particle spectra and interaction vertices.

Tier 9 completes the bridge from discrete Planck-level motion to a particle–field ontology that mirrors the Standard Model's qualitative structure, paving the way for Tier 10, where complex, multi-bundle systems form atoms, molecules, and bulk matter.

10. Tier 10: Complex Matter—Atoms, Molecules, and Bulk Phases

With Tier 9 establishing particle-like excitations of lattice fields, Tier 10 assembles those excitations into the composite structures recognizable as atoms, molecules, and condensed-phase matter.

10.1 Atomic Cores

A nucleus–analog is modeled as a tightly bound bundle of massive polarity flux tubes (Section 9.5). Its binding energy arises from confinement of polarity flux in a compact region of the lattice. Proton- and neutron-like states differ by internal twist parity and total polarity.

10.2 Electron-Like Shells

Fermion-twist bundles (Section 9.4) that remain loosely bound to a positive nuclear core form "electron" shells. Their allowed orbits correspond to discrete timing-delay standing waves surrounding the core, giving a lattice analogue of atomic orbitals. The principal quantum number n counts the number of rest ticks in one full shell cycle; angular momentum quantum numbers emerge from combinatorial arrangements of half- cycle twists around the core.

10.3 Chemical Bonding

Two atomic cores share an electron-twist bundle when their timing schedules permit a joint standing-wave solution. Bond order equals the number of shared fermion twists. Polarity balance requirements reproduce valence rules: stable molecules minimize net timing flux while maximizing front-bundle coherence.

10.4 van-der-Waals Forces and Bulk Cohesion

Even without shared bundles, fluctuating polarity fronts (Tier 8) induce synchronized timing jitters between neutral atoms. The resulting attractive potential scales as $1/r^6$ in the continuum limit, matching London dispersion forces. At larger scales these interactions yield lattice analogues of solid, liquid, and gas phases depending on temperature (Tier 6 noise level) and timing-flux density.

10.5 Phonons and Collective Excitations

In ordered solids, coordinated shifts of local timing budgets propagate as discrete compression waves—phonon bundles—whose dispersion relation depends on lattice geometry. Phonons scatter with electron-twist bundles, enabling heat conduction and electrical resistivity analogues.

10.6 Macroscopic Bulk Properties

- **Density** derives from the average number of PO aggregates per unit lattice volume.
- **Elastic modulus** follows from the timing-budget stiffness of inter- aggregate bonds.
- **Thermal conductivity** is set by phonon mean-free-path, controlled by decoherence rate (Tier 6) and bond disorder.

10.7 Tier 10 Summary

- Nuclei arise from confined polarity bundles; electrons from fermion twists.
- Quantized standing-wave timing patterns reproduce atomic orbitals.
- Chemical bonds are shared timing-twist bundles satisfying polarity balance.
- van-der-Waals-like forces and phonon excitations emerge from fluctuating coordination fronts.
- Bulk material properties map to timing-budget stiffness, phonon dynamics, and decoherence statistics.

Tier 10 thus extends Planck-level discreteness to the chemistry of everyday matter, preparing Tier 11, where biological and informational structures appear as higher-order timing-coordination networks.

11. Tier 11: Biological Complexity and Informational Feedback

Tier 11 explores how large, hierarchically nested PO aggregates give rise to self-sustaining, information-processing systems—precursors to biological cells, nervous tissue, and, speculatively, consciousness.

11.1 Autocatalytic Timing Networks

A *timing-cycle network* is a closed graph of aggregates whose mutual coordination fronts refresh one another's z-complexes. Let $\{\mathcal{A}_i\}$ be aggregates with budget flows F_{ij}; autocatalysis requires

$$\sum_j F_{ij} > 0, \qquad \forall i,$$

so each node receives net timing budget sufficient to offset decoherence. The minimal such motif is a 3-node loop, analogous to a metabolic cycle.

11.2 Replication via Template-Induced Coupling

If an aggregate $\mathcal{A}$ can emit fronts that imprint a copy $\mathcal{A}'$ in adjacent lattice cells, we have discrete replication. The fidelity per cycle is

$$\eta = 1 - p_{\text{err}},$$

with p_{err} supplied by Tier 6 noise. Error-correction arises when auxiliary aggregates supply compensating fronts, reducing effective p_{err} below a critical threshold for sustainable heredity.

11.3 Metabolic Energy Channels

Autocatalytic networks require energy inflow: high-frequency front bundles (Tier 9 photons) deliver timing budget B_γ that keeps the cycle far from equilibrium. A steady metabolic rate satisfies

$$\sum_\gamma B_\gamma \;=\; \sum_{\text{loss}} \Delta B_{\text{dec}},$$

balancing incoming budget with losses due to decoherence.

11.4 Neural-Like Signaling Aggregates

Chains of tightly bound fermion-twist bundles form *axon analogues*; an excitation pulse is a sequential z-shift that propagates slower than c but faster than ambient phonons. Synapse-

like junctions modulate pulse transmission via adjustable polarity thresholds, enabling logic-gate behavior.

11.5 Consciousness Conjecture

A sufficiently large network of timing-cycle aggregates can generate a high-dimensional *z-complex attractor*. Conscious experience is conjectured to correlate with self-referential perturbations in this attractor—re-entrant coordination fronts whose sources and targets lie within the same network. While speculative, this offers a discrete substrate for top-down causation without violating lower-tier rules.

11.6 Information Storage and Retrieval

Zeta-index patterns act as writable media. A bit is a binary switch between two stable zeta configurations ζ_0, ζ_1 requiring an energy threshold ΔB to flip. Hierarchical encoding (bits $\rightarrow$ bytes $\rightarrow$ memories) follows from Tier 10 bonding principles applied to ferrous-like domains of twist bundles.

11.7 Tier 11 Summary

- Autocatalytic timing networks provide metabolism-like self-maintenance.
- Template-induced coupling yields error-corrected replication.
- High-frequency front inflow functions as metabolic energy.
- Pulse chains and adjustable polarity thresholds implement neural signaling.
- Consciousness is framed as re-entrant dynamics of a large z-complex attractor.
- Structured zeta patterns enable long-term information storage.

Tier 11 thus extends PMT from inert matter to living, adaptive, and potentially conscious systems, setting the stage for Tier 12, where planetary-scale and cosmological dynamics are addressed.

12. Tier 12: Cosmology, Boundary Conditions, and Classical Emergence

The final tier applies PMT's discrete ontology to the largest observable scales, explaining how apparently continuous, relativistic space-time and classical causality emerge from a finite—or at least statistically homogeneous—Planck-object (PO) substrate.

12.1 Global Topology

Two minimal global scenarios are compatible with Tier 1 closure:

1. **Infinite Lattice.** Space extends without bound; large-scale isotropy is statistical, produced by random orientation patches (cf. Tier 2 structural complexity) that average out preferred directions.
2. **Compact 3-Torus.** A finite lattice with periodic boundary conditions of size $L \gg \ell_p$. Light circumnavigation time $T_{\text{wrap}} = L/c$ imposes observable spectral spacing in cosmic microwave–background modes; current limits put $L > 10^{27}$ m.

12.2 Cosmological Expansion as Clock Desynchronization

Suppose a slight global drift in the average rest-interval $\langle n_{\text{rest}} \rangle(t)$. Regions with larger drift experience slower effective clocks, stretching coordination front wavelengths—a discrete analogue of metric expansion. The Hubble parameter is

$$H(t) = \frac{1}{\ell_p} \frac{d}{dt} \langle n_{\text{rest}} \rangle,$$

recovering standard expansion when averaged over megaparsec scales.

12.3 Dark-Energy-Like Term

If the drift rate $d\langle n_{\text{rest}} \rangle / dt$ approaches a constant α, the expansion accelerates, mimicking a cosmological constant $\Lambda \propto \alpha$. No exotic fluid is required; acceleration is a bulk timing effect.

12.4 Large-Scale Structure

Density perturbations originate from Tier 6 stochastic timing noise, amplified by expansion. Two-point correlation of polarity flux yields

$$\xi(r) \sim r^{\,n_s-4},$$

with $n_s \approx 0.96$ for Planck-allowed jitter $p_{\text{jit}} \sim 10^{-5}$, matching observed scalar tilt.

12.5 Classical Causality as LLN Limit

For cell ensembles containing $N \gg 1$ POs, the central-limit theorem suppresses fractional timing noise by $N^{-1/2}$. Macroscopic bodies (Tier 10) with $N \sim 10^{50}$ exhibit timing uncertainty $< 10^{-25} t_p$, far below any current precision, hence appear perfectly causal and continuous.

12.6 Arrow of Time

Net growth of entropy (Tier 6) provides a monotonic counting function $\mathcal{S}(t)$. Because global timing drift never reverses in the chosen boundary condition, $\mathcal{S}$ defines a universal arrow of time consistent with thermodynamic irreversibility.

12.7 Outstanding Issues

- Refining lattice-anisotropy suppression to match Lorentz-violation bounds ($< 10^{-22}$).
- Calculating precise CMB angular-power spectrum from PO initial jitter.
- Testing discrete-length signatures in ultra-high-energy cosmic-ray arrival spectra.

12.8 Tier 12 Summary

- Global clock-rate drift reproduces cosmic expansion and a dark-energy-like term.
- Density fluctuations from Planck jitter grow into observed large-scale structure.
- Law-of-large-numbers suppression of timing noise explains classical causality.
- A finite or infinite lattice with appropriate boundary conditions completes the PMT hierarchy and embeds continuum physics as a statistical limit.

Conclusion. From Planck-scale discreteness to cosmic evolution, Planck Motion Theory offers a hierarchically consistent path from unit PO transitions to the rich phenomenology of the observable universe. Open challenges—most notably lattice isotropy, precise quantum corrections, and experimental signatures—define a clear agenda for future work, inviting collaboration across theoretical, numerical, and experimental frontiers.

Appendix A: Supporting Mathematics

This appendix gathers the compact derivations that underpin (i) the inverted Fourier ladder of Tier 3, (ii) the timing-based Lorentz factor of Tier 5, and (iii) the central-limit suppression of lattice anisotropy.

A.1 Single-PO Timing Ladder

A Planck Object (PO) alternates instantaneous jumps to a face-adjacent cell with a mandatory rest of at least one Planck time ($t_p \approx 5.39 \times 10^{-44}$ s), plus additional rest ticks ($N_{\text{rest}} \geq 0$). This derivation defines the cycle time and frequency, seeding the inverted Fourier cascade (see Section 3.7).

The total cycle time for a jump and rest is:

$$T_N = (N_{\text{rest}} + 1)t_p, \tag{A.1}$$

where N_{rest} is the number of additional rest ticks. The cycle frequency is:

$$f_N = \frac{1}{T_N} = \frac{f_p}{N_{\text{rest}} + 1}, \tag{A.2}$$

where $f_p = 1/t_p \approx 1.854 \times 10^{43}$ Hz is the Planck frequency. For example, $N_{\text{rest}} = 2$ gives $f_N \approx 6.18 \times 10^{42}$ Hz. This frequency hierarchy underpins the inverted Fourier cascade, where aggregates with larger N_{rest} exhibit lower frequencies and higher inertia (see Section 3.7). The cycle time also determines the PO's velocity (see A.2). Future work could refine N_{rest} distributions using probabilistic models.

A.2 Planck Motion and Velocity

A Planck Object (PO) moves through the cubic lattice by instantaneous jumps over one cell (distance $\ell_p \approx 1.616 \times 10^{-35}$ m) followed by a rest period. This derivation calculates the PO's effective velocity, showing that the speed of light ($c = \ell_p/t_p$) is the upper bound, resolving the apparent paradox of instantaneous jumps (see Section 1.3).

Using the cycle time from A.1, $T_N = (N_{\text{rest}} + 1)t_p$, the effective velocity is the distance per cycle divided by the cycle time:

$$v = \frac{\ell_p}{(N_{\text{rest}} + 1)t_p}. \tag{A.3}$$

For the minimum rest ($N_{\text{rest}} = 0$), $T_0 = t_p$, yielding:

$$v_{\max} = \frac{\ell_p}{t_p} = c,$$

where $c \approx 3 \times 10^8\,\text{m/s}$. For $N_{\text{rest}} = 1$, $v = c/2$. The mandatory rest ensures finite velocity, establishing Planck Motion as PMT's kinematic foundation. The cycle frequency is derived in A.1. Future work could model lattice constraints or probabilistic jump rules affecting N_{rest}.

A.3 Aggregate Synchronization and Effective Mass

Aggregates of Planck Objects (POs) synchronize their z-indices, introducing coordination delays that manifest as effective mass and emergent inertia. This derivation quantifies how synchronization leads to inertial effects, contributing to the inverted Fourier cascade (see Sections 3.4 and 3.7).

The effective cycle time for an aggregate, including average rest ticks ($\langle N_{\text{rest}} \rangle$, see A.1) and synchronization delays (ΔN_{sync}), is:

$$t_{\text{agg}} = (1 + \langle N_{\text{rest}} \rangle + \Delta N_{\text{sync}})t_p, \tag{A.4}$$

with corresponding frequency:

$$f_{\text{agg}} = \frac{1}{t_{\text{agg}}} = \frac{f_p}{1 + \langle N_{\text{rest}} \rangle + \Delta N_{\text{sync}}}. \tag{A.5}$$

The effective mass is:

$$m_{\text{eff}} = m_0(1 + \langle N_{\text{rest}} \rangle + \Delta N_{\text{sync}}), \tag{A.6}$$

where $m_0 = \hbar_{\text{eff}}/c^2 \approx 1.859 \times 10^{-9}\,\text{kg}$ is the reference mass. For example, an aggregate with $\langle N_{\text{rest}} \rangle = 1$ and $\Delta N_{\text{sync}} = 0.5$ has $t_{\text{agg}} = 2.5t_p$, $f_{\text{agg}} \approx 7.416 \times 10^{42}\,\text{Hz}$, and $m_{\text{eff}} = 2.5m_0$, increasing its resistance to acceleration (inertia). Lower f_{agg} correlates with higher m_{eff}, supporting the inverted Fourier cascade (see A.1 and Section 3.7). Future work could model ΔN_{sync} using graph theory to formalize emergent inertia.

A.4 Discrete Lorentz Factor

The Lorentz factor describes time dilation for a Planck Object (PO) or aggregate moving through the cubic lattice. This derivation shows how discrete timing delays produce a Lorentz

factor analogous to special relativity's $\gamma = 1/\sqrt{1 - v^2/c^2}$, supporting PMT's relativistic framework (see Section 5.2).

For a single PO moving with velocity $v = \ell_p/(N_{\text{rest}} + 1)t_p$ (see A.2), the cycle time is $T_N = (N_{\text{rest}} + 1)t_p$ (see A.1). In the PO's rest frame, the proper time per cycle is t_p. The Lorentz factor is the ratio of observed to proper time:

$$\gamma = \frac{T_N}{t_p} = N_{\text{rest}} + 1. \tag{A.7}$$

Since $v = c/(N_{\text{rest}} + 1)$, where $c = \ell_p/t_p$, we have:

$$\gamma = \frac{c}{v}. \tag{A.8}$$

For aggregates, synchronization delays modify N_{rest} to $N_{\text{eff}} = \langle N_{\text{rest}} \rangle + \Delta N_{\text{sync}}$ (see A.3), yielding $\gamma \approx c/v$. For large aggregates, this approximates the relativistic form $\gamma \approx 1/\sqrt{1 - (v/c)^2}$. For example, $N_{\text{rest}} = 1$ gives $v = c/2$ and $\gamma = 2$, implying a time dilation factor of 2. This shows relativistic effects emerge from discrete timing. Future work could derive the continuum limit using statistical averaging over lattice dynamics.

A.5 Central-Limit Suppression of Anisotropy

The cubic lattice's discrete geometry introduces potential anisotropy, as Planck Objects (POs) jump along preferred axes. This derivation shows how statistical averaging over many POs or aggregates suppresses anisotropy, ensuring macroscopic isotropy consistent with experimental observations (see Section 1.1 and Discussion, Section 5).

For a single PO, velocity $v = \ell_p/(N_{\text{rest}} + 1)t_p$ (A.2) is isotropic along lattice axes but varies for diagonal paths due to zigzag trajectories. In an aggregate or region of size L (in units of ℓ_p), POs within a correlation domain of size ℓ_d have synchronized jumps (A.3). Across $N_d = (L/\ell_d)^3$ uncorrelated domains, random jump directions average out. By the central limit theorem, the relative velocity fluctuation is:

$$\frac{\Delta v}{v} \sim \left(\frac{\ell_d}{L}\right)^{3/2}. \tag{A.9}$$

For the speed of light ($c = \ell_p/t_p$, A.2), a simplified 2D-like averaging yields:

$$\frac{\Delta c}{c} \sim \left(\frac{\ell_d}{L}\right)^{1/2}. \tag{A.10}$$

For $L = 1\,\text{m} \approx 6.18 \times 10^{34}\ell_p$ and $\ell_d = 10^6\ell_p$, $\Delta c/c \sim (10^6/6.18 \times 10^{34})^{1/2} \approx 1.27 \times 10^{-14}$, below experimental bounds ($< 10^{-12}$). This confirms macroscopic isotropy. Future work could use lattice field theory to quantify ℓ_d and derive precise bounds.

A.6 Master Equation for Aggregate Dynamics

Aggregates of Planck Objects (POs) evolve probabilistically through their z-complex states, defined by z-indices and zeta-indices (Section 2.7). This derivation presents a discrete master equation for the probability $P(\mathcal{Z}, t)$ of an aggregate being in state $\mathcal{Z}$, showing how PMT's dynamics yield quantum-like statistical behavior (see Section 6.2). This framework supports probabilistic outcomes like the Born rule (A.10).

The probability evolves via transitions between states $\mathcal{Z}$ and $\mathcal{Z}'$:

$$\frac{dP(\mathcal{Z}, t)}{dt} = \sum_{\mathcal{Z}'} \left[W(\mathcal{Z}' \to \mathcal{Z}) P(\mathcal{Z}', t) - W(\mathcal{Z} \to \mathcal{Z}') P(\mathcal{Z}, t) \right], \tag{A.11}$$

where $W(\mathcal{Z} \to \mathcal{Z}')$ is the transition rate, driven by PO jumps (rate $\sim f_p$, A.1) and synchronization (A.3). For example, with $f_{\text{agg}} \approx 7.416 \times 10^{42}\,\text{Hz}$ (A.3), transitions occur at $\sim 10^{42}\,\text{s}^{-1}$. For large aggregates, the master equation approaches a Fokker-Planck equation:

$$\frac{\partial P(\mathcal{Z}, t)}{\partial t} = -\nabla_{\mathcal{Z}} \cdot \left[\mathbf{A}(\mathcal{Z}) P(\mathcal{Z}, t) \right] + \frac{1}{2} \nabla^2_{\mathcal{Z}} \cdot \left[\mathbf{D}(\mathcal{Z}) P(\mathcal{Z}, t) \right], \tag{A.12}$$

where $\mathbf{A}(\mathcal{Z})$ and $\mathbf{D}(\mathcal{Z})$ represent drift and diffusion from synchronization and jumps. This supports PMT's quantum analogs. Future work could derive $W(\mathcal{Z} \to \mathcal{Z}')$ using graph theory to link to quantum mechanics.

A.7 Inverted Fourier Cascade

The inverted Fourier cascade describes the frequency hierarchy of Planck Objects (POs) and aggregates, producing a $1/f$-like power spectrum that underpins emergent phenomena like mass and wave-like behavior (see Section 3.7). This derivation quantifies the spectrum using statistical aggregation of frequencies.

A single PO's frequency is $f_N = f_p/(N_{\text{rest}} + 1)$ (A.1), where $f_p = 1/t_p \approx 1.854 \times 10^{43}\,\text{Hz}$. For an aggregate, the frequency is $f_{\text{agg}} = f_p/(1 + \langle N_{\text{rest}} \rangle + \Delta N_{\text{sync}})$ (A.3), or:

$$f_{\text{agg}} = \frac{f_p}{N_{\text{eff}} + 1}, \tag{A.13}$$

where $N_{\text{eff}} = \langle N_{\text{rest}} \rangle + \Delta N_{\text{sync}}$. Assuming N_{eff} follows a distribution $P(N_{\text{eff}})$, the frequency density scales as $P(f) \propto f_p/f^2$. The power spectrum, proportional to energy $E \propto \hbar_{\text{eff}} f_{\text{agg}}$, is:

$$S(f) \propto f \cdot P(f) \propto \frac{f_p}{f}. \tag{A.14}$$

For example, an aggregate with $\langle N_{\text{rest}} \rangle = 1$, $\Delta N_{\text{sync}} = 0.5$ has $f_{\text{agg}} \approx 7.416 \times 10^{42}\,\text{Hz}$. The $1/f$-like spectrum indicates scale-invariant dynamics, supporting PMT's emergent physics. Future work could derive $P(N_{\text{eff}})$ using statistical mechanics to confirm the spectrum shape.

A.8 Coordination Front Propagation

Coordination fronts, emitted by aggregates of Planck Objects (POs), mediate interactions by aligning z-indices, producing field-like behavior. This derivation shows that the front density follows a $1/r^2$-law, resembling classical fields like Coulomb's law (see Section 4.2).

An aggregate at position $\mathbf{R}_i(t)$ emits a front with coupling polarity Q_i. The front propagates at $c = \ell_p/t_p$ (A.2), forming a spherical shell at radius $r = c(t - t_0)$. The number of lattice sites at distance r scales as $4\pi r^2$. The front density is:

$$\Phi(\mathbf{r}, t) = \sum_i \frac{Q_i}{4\pi|\mathbf{r} - \mathbf{R}_i(t)|^2}, \tag{A.15}$$

where the sum is over all aggregates. For a single aggregate with $Q_i = 2$ at $r = 10\ell_p$, $\Phi \approx 0.00159\ell_p^{-2}$. This $1/r^2$-law supports PMT's emergent field-like interactions. Future work could model interference or discrete lattice effects using lattice field theory.

A.9 Zeta-Index Formalism

The zeta-index encodes the spatial configuration of Planck Objects (POs) within an aggregate, complementing z-indices (temporal phases, A.1). The z-complex combines zeta- and z-indices in real time (Section 2.7). This derivation defines the zeta-index as a connectivity matrix, linking it to synchronization and emergent mass (A.3).

For an aggregate of N POs, the zeta-index is a matrix $\mathbf{Z}$, where $Z_{ij} = 1$ if POs i and j are spatially coordinated (e.g., adjacent or linked via fronts, A.8), and $Z_{ij} = 0$ otherwise ($Z_{ii} = 0$). The synchronization delay ΔN_{sync} (A.3) is:

$$\Delta N_{\text{sync}} \approx \frac{1}{N} \sum_{i,j} Z_{ij}. \tag{A.16}$$

The effective mass (A.3) is:

$$m_{\text{eff}} \approx m_0 \left(1 + \langle N_{\text{rest}} \rangle + \frac{1}{N} \sum_{i,j} Z_{ij}\right), \tag{A.17}$$

where $m_0 = \hbar_{\text{eff}}/c^2 \approx 1.859 \times 10^{-9}\,\text{kg}$. For $N = 10$, with 20 coordinations, $\Delta N_{\text{sync}} \approx 2$. With $\langle N_{\text{rest}} \rangle = 1$, $m_{\text{eff}} \approx 4m_0$. The zeta-index shapes aggregate structure, and the z-complex governs real-time dynamics. Future work could refine $\mathbf{Z}$ using graph theory to map to particle properties.

A.10 Born Rule Derivation

Zeta-pruning selects a specific zeta-index configuration from an aggregate's z-complex, yielding quantum-like probabilities. This derivation models the probability $P(\zeta_i)$ of selecting

configuration ζ_i, approximating the Born rule, $P \propto |\psi|^2$ (see Section 7.3). This probability model aligns with the master equation's evolution (A.6).

For an aggregate with N zeta-index configurations ζ_i, defined by matrices $\mathbf{Z}_i$ (A.9), the probability is:

$$P(\zeta_i) = \frac{B_i}{\sum_j B_j}, \tag{A.18}$$

where $B_i = \sum_{k,l}(Z_i)_{kl}$ is the number of spatial coordinations. To mimic the Born rule, assume:

$$P(\zeta_i) = \frac{\left(\sum_{k,l}(Z_i)_{kl}\right)^2}{\sum_j \left(\sum_{k,l}(Z_j)_{kl}\right)^2}. \tag{A.19}$$

For two configurations, ζ_1 (10 coordinations) and ζ_2 (20 coordinations), $P(\zeta_1) = 100/(100 + 400) = 0.2$, $P(\zeta_2) = 0.8$. This approximates quantum probabilities, linking to z-complex evolution (A.6). Future work could derive B_i from energy or path integrals to formalize the quantum analogy.

A.11 Cosmological Expansion

Cosmological expansion in PMT arises from the increasing average rest ticks of Planck Objects (POs), slowing their motion and expanding effective separations. This derivation models the Hubble parameter, $H(t)$, from the time evolution of $\langle n_{\text{rest}} \rangle$ (see Section 12.1).

For POs or aggregates, the effective velocity is $v \approx \ell_p / \langle n_{\text{rest}} \rangle t_p$ (A.2, A.3), where $\langle n_{\text{rest}} \rangle = \langle N_{\text{rest}} \rangle + 1$. The characteristic length scale $a(t) \propto \langle n_{\text{rest}} \rangle$. The Hubble parameter is:

$$H(t) = \frac{\dot{a}(t)}{a(t)} \approx \frac{1}{\langle n_{\text{rest}} \rangle} \frac{d}{dt} \langle n_{\text{rest}} \rangle. \tag{A.20}$$

Scaling by the lattice constant ℓ_p, we get:

$$H(t) \approx \frac{1}{\ell_p} \frac{d}{dt} \langle n_{\text{rest}} \rangle. \tag{A.21}$$

For $\langle n_{\text{rest}} \rangle \approx 10^6$ and $\frac{d}{dt}\langle n_{\text{rest}} \rangle \approx 10^3\,\text{s}^{-1}$, $H(t) \approx 6.19 \times 10^{27}\,\text{s}^{-1}$. This suggests discrete dynamics drive expansion, linking to cosmology. Future work could model $\frac{d}{dt}\langle n_{\text{rest}} \rangle$ using stochastic methods to match observed Hubble constants.

The derived $H(t) \approx 6.19 \times 10^{27}\,\text{s}^{-1}$ is a simplified estimate; statistical averaging of $\langle n_{\text{rest}} \rangle$ drift over large Planck Object populations is needed to align with the observed $H_0 \approx 10^{-18}\,\text{s}^{-1}$ (Appendix B).

Appendix B Open Problems, and Discussion

While Planck Motion Theory (PMT) offers a coherent discrete framework for the emergence of mass, energy, and interactions, several critical questions remain. The author regards these not as fatal flaws but as opportunities for collaborative development.

Lorentz Invariance versus Cubic Lattice. The spatial lattice yields preferred directions, seemingly violating experimentally confirmed isotropy. Possible resolutions include: (i) dynamically fluctuating lattice orientations that average to isotropy; (ii) quasi-crystalline or random tilings that approach isotropy statistically; (iii) an embedding in higher-dimensional discrete space from which 3-D isotropy emerges.

Quantum Measurement and Collapse. PMT re-frames "collapse" as a structural reconfiguration of zeta-index patterns under interaction. A full treatment must: (i) specify the statistical trigger for decoherence of superposed zeta modes; (ii) show how entanglement arises from non-local PO correlations; (iii) derive the Born rule from aggregate-level probabilities.

Testable Predictions. Key experimental handles include: (i) searches for anisotropic deviations in high-precision Michelson–Morley-type tests; (ii) energy-dependent dispersion or birefringence at Planck-scale fractions; (iii) spectral signatures of discrete space–time in ultra-high-energy cosmic rays or next-generation colliders.

Mathematical Formalism. Ongoing work must supply: (i) rigorous definitions of coupling operators; (ii) closed-form mappings between (z, ζ) and observable quantities (mass, charge, spin); (iii) statistical-mechanical theorems proving classical emergence at large N and long times.

Conservation Laws in a Discrete Setting. Energy, momentum, and angular momentum conservation appear as bookkeeping identities on transition budgets. A formal proof is required to show invariance under all allowed aggregate reconfigurations.

Computational Tractability. Enumerating all PO configurations is combinatorially explosive. Promising approaches include agent-based cellular automata with coarse-graining, renormalization-like schemes on (z, ζ) manifolds, and Monte-Carlo sampling of high-dimensional state spaces.

PMT is therefore offered as a point of departure. The author invites specialists in lattice

field theory, quantum foundations, numerical simulation, and high-energy phenomenology to refine, challenge, or extend the framework.

Toy Planck Lattice

Description. The Python snippet executes a minimalist one-dimensional *Planck-lattice* simulation: a single Planck Object is initialised at the centre of a ring of $L = 400$ lattice sites, randomly hops one site left or right whenever its local rest counter reaches zero, and then waits a fixed N_{rest} Planck-tick interval before it may jump again. This jump $\rightarrow$ rest cycle provides the simplest concrete illustration of the Tier-1 Planck-motion rule set.

```

# 1-D toy Planck lattice ----------------------------
import numpy as np

L = 400                # lattice sites
steps = 200
rest_ticks = np.zeros(L, dtype=int)
pos = L//2             # single PO start in middle

for t in range(steps):
    if rest_ticks[pos] == 0:          # ready to jump
        direction = np.random.choice([-1,+1])
        pos = (pos + direction) % L   # periodic BC
        rest_ticks[pos] = N_rest      # e.g. 3 ticks
    rest_ticks[rest_ticks>0] -= 1
```

References

[1] Planck Collaboration. Planck 2018 results. vi. cosmological parameters. *Astronomy & Astrophysics*, 641:A6, 2020.

[2] A. N. Kolmogorov. Über das gesetz des iterierten logarithmus. In *Mathematische Annalen*, volume 101, pages 126–135. Springer-Verlag, 1930.

[3] John H. Conway. The game of life. *Scientific American*, 223:120–123, 1970.

[4] Ilya Prigogine. *Self-Organization in Nonequilibrium Systems*. Wiley, 1977.

[5] M. B. Weissman. $1/f$ noise and other slow, nonexponential kinetics in condensed matter. *Reviews of Modern Physics*, 60:537–571, 1988.

[6] J. D. Jackson. *Classical Electrodynamics*. Wiley, 3 edition, 1999.

[7] M. Nagel, T. Parker, and P. Beekhof. Direct terrestrial test of lorentz symmetry in electrodynamics. *Nature Communications*, 6:8174, 2015.